Available online at www.sciencedirect.com
ScienceDirect
Cement & Concrete Composites 29 (2007) 700–711
Cement & Concrete Composites
www.elsevier.com/locate/cemconcomp

Repair evaluation of concrete cracks using surface and through-transmission wave measurements

D.G. Aggelis, T. Shiotani *

Research Institute of Technology, Tobishima Corporation, 5472 Kimagase, Noda, Chiba 270-0222, Japan

Received 26 October 2006; received in revised form 14 April 2007; accepted 2 May 2007
Available online 13 May 2007

Abstract

Surface opening cracks are common defects in large civil structures like bridges. They allow penetration of water or other agents that result in loss of durability earlier than expected. Their repair can be conducted by the injection of epoxy material that seals the crack sides keeping out any aggressive substances in addition to the recovery of strength. In order to evaluate crack parameters before impregnation as well as to determine the final repair effectiveness, a combination of Rayleigh and longitudinal waves is applied. Rayleigh waves demonstrate the filling condition of the material into the shallow layer near the surface while tomography using longitudinal waves through the thickness yields information about the area inside the structure. Wave propagation dispersion features are exploited by the proposed tomography at different frequencies, demonstrating that higher frequencies lead to more accurate characterization.

Keywords: Concrete; Characterization; Cracks; Repair; Ultrasound

1. Introduction

Surface-breaking cracks belong probably to the most commonly seen kind of defects in civil structures. They may occur due to the combined effect of overloading, drying shrinkage, temperature variations, chemical attacks, weathering, differential settlement and other degradation processes. The most important consequence is the exposure of the metal reinforcement to environmental parameters that lead to its accelerated oxidation [1–7] and finally the loss of durability of the structure.

Materials technology has made significant progress to provide solutions to many shortcomings arising in civil structures. Materials with superior mechanical properties and resistance to corrosion enable different effective repair techniques. Common methods of repair include epoxy or grout injection [7–10] and surface applications of fiber reinforced polymer strips [10].

Stress waves offer a non-invasive means of crack characterization and have been used for such cases in order to evaluate crack parameters. Wave characteristics such as the transit time [6,11,12], the energy or energy related parameters [5,13] and frequency content [3,14] provide an estimation of crack depth. Also, numerical simulations have enhanced the understanding of Rayleigh waves interacting with surface-breaking cracks [14,15]. However, the present case of investigation differs from the above in the respect that the cracks were through the thickness and therefore, there was no need for depth measurement. Specifically, the cracks developed through the concrete bridge deck. The cause is supposed to be the combined effect of shrinkage and premature removal of the mechanical support, which led to overloading before adequate hardening of the material. Therefore, the inspection was conducted using a combination of longitudinal and Rayleigh waves before, as well as after injection of epoxy in order to ensure the work effectiveness. The important issue was the evaluation of repair effectiveness after epoxy injection.

* Corresponding author. Tel.: +81 4 7198 7572; fax: +81 4 7198 7586.
E-mail address: tomoki_shiotani@tobishima.co.jp (T. Shiotani).

0958-9465/$ - see front matter © 2007 Elsevier Ltd. All rights reserved.
doi:10.1016/j.cemconcomp.2007.05.001

2. Rayleigh waves

The use of Rayleigh (or surface) waves seems quite suitable for surface opening cracks investigation, since they propagate along the surface of the structure. Additionally, they occupy higher percentage of energy than the other types of waves. For example, as mentioned in [3] a point source in a homogeneous half space radiates 67% of its energy in the form of Rayleigh waves, while only 7% in compressional ones. Moreover, since they are essentially two-dimensional, their energy does not disperse as rapidly as the energy associated with three-dimensional dilatational and shear waves [16]. Specifically, their amplitude is inversely proportional to the square root of propagation distance while for a longitudinal wave the amplitude is inversely proportional to the distance [17]. This makes them more easily detectable than other kinds of waves. The particle motion is elliptical and at the surface the vertical component is greater than the horizontal. The motion decreases exponentially in amplitude away from the surface [16].

More specifically, the penetration depth of these waves is considered to be similar to their wavelength [2,6]. Using the expressions for the out-of-plane displacements for Rayleigh waves as given for example in [18], one can obtain accurate values of the amplitude with respect to the penetration depth. In Fig. 1, the vertical to the surface amplitude vs the penetration depth of Rayleigh waves for two different frequencies is depicted. In this example the material is assumed to be sound concrete with longitudinal wave velocity $C_p = 5000$ m/s and shear velocity $C_s = 3000$ m/s. The Rayleigh velocity for this case is $C_R = 2745$ m/s. It can be calculated that at the depth of one wavelength the amplitude of the Rayleigh wave has almost completely decayed (6% compared to the amplitude at the surface). For the case of 30 kHz this happens at approximately the depth of 91 mm and for 100 kHz at the depth of 27 mm.

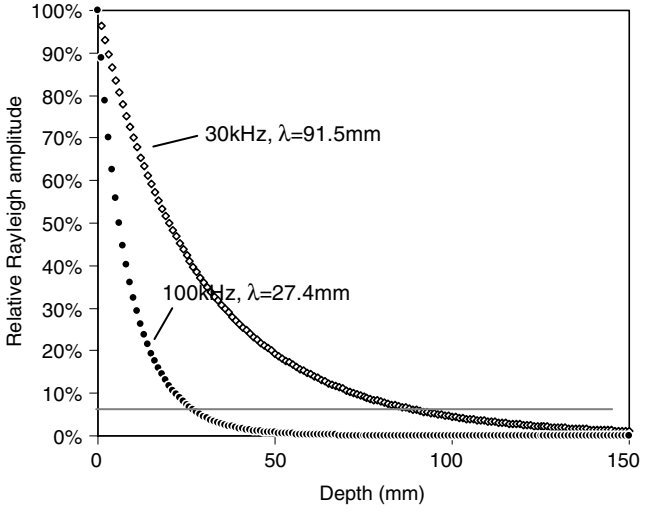

Fig. 1. Out-of-plane amplitude of Rayleigh waves vs depth of penetration for different frequencies.

In case of a surface opening crack, the transmission and the frequency of the wave passing through the crack will diminish as the crack depth increases [19], up to a point that no energy in the form of Rayleigh waves will be transmitted any more for large crack depth [20–22]. Therefore, a crack of 30 mm depth would block almost entirely the propagation of the 100 kHz surface wave, while it would allow an amount of the energy of 30 kHz. This illustrates that frequency is a decisive factor for inspection with Rayleigh waves. This feature has been extensively used to asses the quality of different layers of concrete [2,11,23–25], since high frequency components propagate only along the shallow portion of the structure while the lower frequency ones propagate also in deeper layers and thus their propagation velocity is affected by their properties as well.

In addition to surface waves measurements, since there was access to both sides of the deck in the particular case described herein, measurements were conducted also using longitudinal waves through the thickness with application of tomography, a technique commonly used for evaluation of the interior of structures [7,8,26] originated from geophysics [27].

3. Repair and measurements details

The task faced in such a case is twofold; first the estimation of crack parameters and second the assessment of the repair effect. In the present case, since the cracks were through the thickness, they were visible from both top and bottom sides of the deck and thus, their depth was equal to the thickness of the concrete deck. Therefore, the most important task was the estimation of the improvement effect after repair.

The engineers at site selected a specific epoxy for injection with a density of 1.15 g/cm^3, curing time of 30 min and a final modulus of elasticity of 1 GPa. It is noted that the concrete material used at the bridge site had a water to cement ratio of 0.43, and maximum aggregate size of 20 mm. Epoxy was applied from the top surface at several points along each crack opening by means of syringes with rubber strips applying a pressure of 1 kg/cm^2.

The objective of this repair method is to fill the crack and bond the concrete on both sides of the crack. In this way water, chlorides and other aggressive substances are kept out while structural strength is also provided [1]. The consumed quantity of epoxy was available by the site log data. However, since the internal pattern of the crack is not known, it was not possible to estimate how successful the impregnation was. Ultrasonic wave measurement and analysis were conducted for all cracks, whereas in this paper an indicative case will be described. The crack width at the surface was 0.2 mm.

The experimental arrangement can be seen in Fig. 2. Totally 10 sensors were used; five on each surface in a way that the crack was between the 8th and 9th on the upper side, while the array was parallel to the axis of the structure. The sensors used were acoustic emission R6,

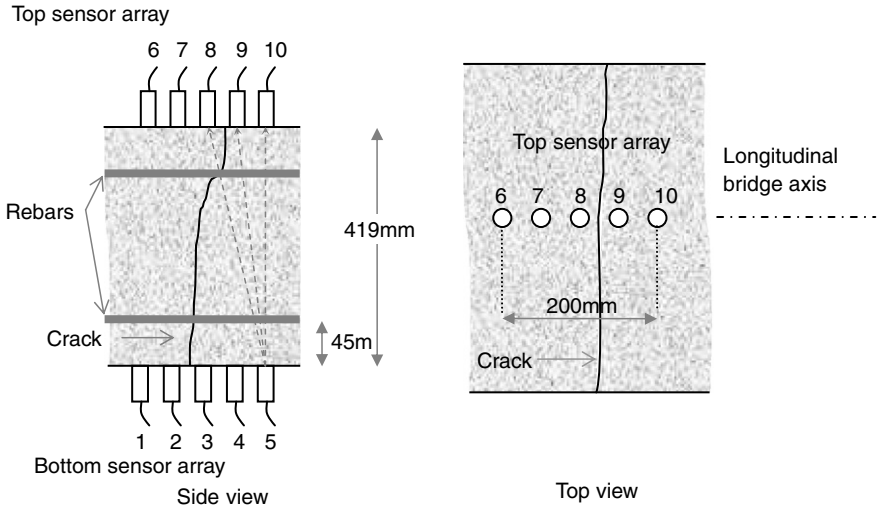

Fig. 2. Schematic representation of sensor arrangement.

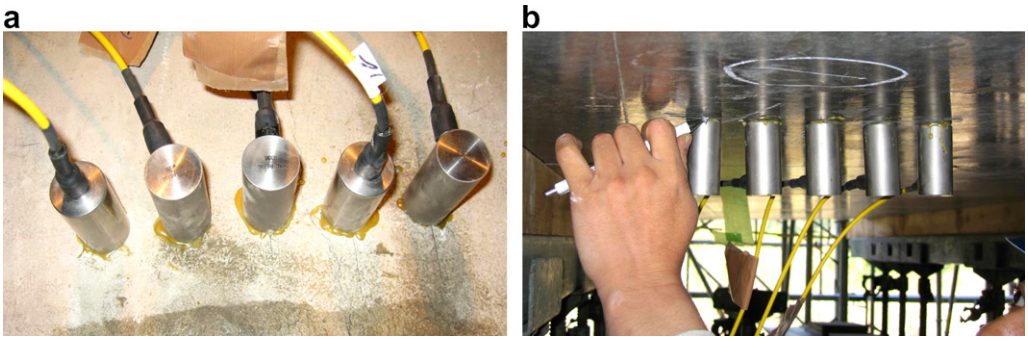

Fig. 3. (a) Photograph of sensor arrangement of the upper side and (b) excitation using lead break and sensor at the down side.

Physical Acoustics Corp. They nominally exhibit high sensitivity at bands around 100 kHz. The data acquisition system was an acoustic emission monitoring multi-channel PAC DISP, while the sampling rate was set to 10 MHz. Different kinds of excitation were used; namely pulse generator, ball impact of diameter 8 mm and pencil lead break. The most reliable results were obtained by the lead excitation and these are reported in this work. This way, a quite wideband excitation is accomplished since frequencies up to 200 kHz are generated. The sensors were attached to the surface using melted electron wax as seen in Fig. 3a. Excitation was applied at each sensor position consecutively, see Fig. 3b. The waveforms received from the sensors of the same side were used for the Rayleigh wave analysis, while from the opposite side are used for the tomography that will be described later.

4. One-sided measurements

4.1. One-sided wave measurements

As stated in the introduction a straight-forward way to determine the depth of a crack is the measurement of the transit time of the wave diffracted by the tip of the crack, see Fig. 4a. This configuration was used (similar as in [6]) in order to estimate the difference between cracked and repaired state. The transit time of the signal, see Fig. 4b for the case before repair, corresponds to the depth of 59.5 mm, although the metal reinforcement depth is 45 mm. Therefore, it is possible that the actual onset of the diffracted wave through the rebar was weak enough and not detectable. After the impregnation with epoxy, similar measurement led to the waveform that can also be seen in Fig. 4b. An increase of energy is expected [28] since stress waves pass also through the zone provided by the repair agent. Apart from the apparently higher energy transmitted, the onset is much earlier, corresponding to a crack depth of 23 mm. However, an empty portion of that size and at that point is not likely, since the injection was conducted by the same surface that also the wave measurements were conducted. This result should be attributed to the fracture process zone that affects the longitudinal as well as the Rayleigh waves and is discussed in the next section. Anyway, it was obvious in the specific case that using the conventional one-sided ultrasonic measurement of the diffracted wave, crack properties could not be evaluated.

Therefore, additional measurements based on Rayleigh waves were conducted. As a reference, the measurement

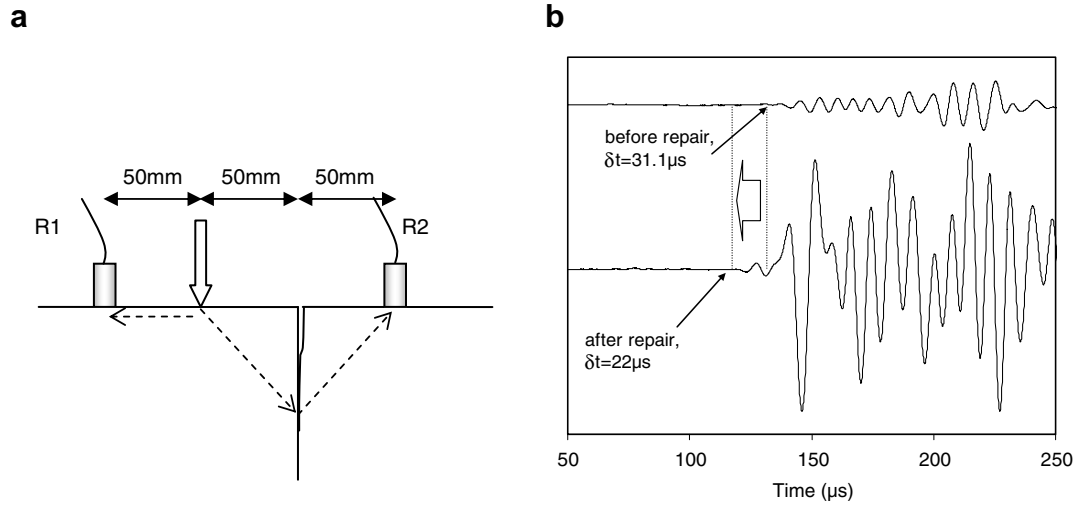

Fig. 4. (a) Schematic representation of one-sided crack depth measurements and (b) waveforms of the receiver after the crack (R2).

was first conducted on sound material. In Fig. 5a the response at different distances from the excitation can be seen. Near the impact, the amplitude is too strong and therefore is saturated; however this does not cause considerable experimental scatter in the determination of the peak time as will be seen in Fig. 5b. The Rayleigh wave is generally easily detectable since it corresponds to a strong peak following the first arrival of the longitudinal wave which is of certainly lower amplitude [6,29]. Plotting the arrival time of the peak with respect to distance, as seen in Fig. 5b, yields the propagation velocity which is the slope of the line. Since the material is sound with no defects, there is no variation in the Rayleigh velocity and according to the distance, the peaks' arrivals is strongly correlated with the time. The high Rayleigh velocity of about 2660 m/s is indicative of the sound internal condition of the material that has not yet suffered any deterioration. Indeed, the P-wave velocity was measured at around 5000 m/s, a value which, according to empirical correlations, implies very high quality material.

When the same sensor configuration was used to measure a portion containing a crack, different trends were observed, as shown in Fig. 6. The first three waveforms, collected before the crack, are quite clear, while after the crack the waveforms are hardly visible. This shows that a very small part of energy is transmitted through the crack. In Fig. 7a the same waveforms are depicted, with the two waveforms after the crack magnified by a factor of 20. It is obvious that no peak corresponds to the Rayleigh velocity of the material. Plotting the arrival time vs distance using the peaks closest to the expected time for the two last waveforms, results in weaker correlation as seen in Fig. 7b. Therefore, it seems that the Rayleigh wave does not survive after the crack, due to the discontinuity.

The same configuration was used to evaluate the condition after injection. The waveforms are depicted in Fig. 8a.

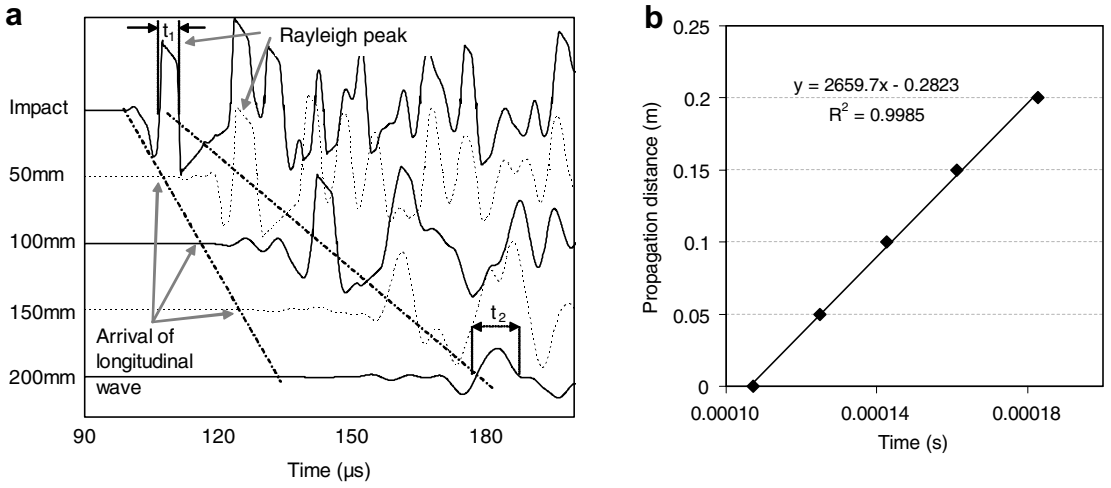

Fig. 5. (a) Waveforms of surface measurements at different propagation distances for sound concrete and (b) correlation plot of distance to Rayleigh peak arrival time.

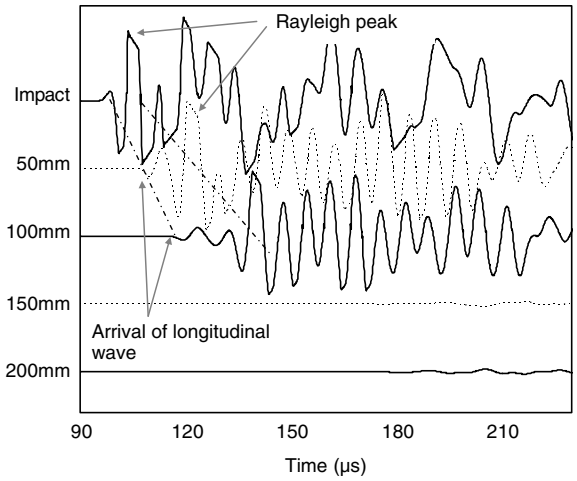

Fig. 6. Waveforms of surface measurements at different propagation distances for concrete with crack at 125 mm.

It is obvious that more energy is transmitted than before repair. The Rayleigh peaks can be distinguished due to their larger height after the initial P-wave arrivals even at the measurement points after the crack. Moreover, in Fig. 8b the correlation is almost as strong as the sound case of Fig. 5b, verifying that these peaks correspond to surface waves. Nevertheless, the velocity is calculated at 2414 m/s, about 250 m/s lower than the corresponding velocity of the sound material, most likely due to the propagation through the layer of epoxy inside the crack. This means that the last two points, corresponding to propagation of 150 mm and 200 mm are somewhat delayed. Indeed, excluding these points from the correlation, see the dashed grey line of Fig. 8b, leads to a velocity of 2605 m/s and an even higher correlation coefficient, $R^2 = 0.9994$. The lower velocity of 2414 m/s is certainly attributed to the repaired crack situation although the crack width is very small. As mentioned earlier, the crack width at the top was measured at 0.2 mm and the receiver array covered a space of 200 mm. Considering a Rayleigh velocity of 2600 m/s for concrete and 700 m/s for epoxy, propagation through 199.8 mm of concrete and 0.2 mm of epoxy, would result in a measured velocity of 2597 m/s. This difference is too small (of the order of 0.12%) within errors arising from the sampling rate and the positioning of the sensors. However, the actually measured velocity drop is much greater (about 10% or more). The reason for the larger than expected decrease should be sought in the influence of the fracture process zone, which expands several cm away from both sides of the crack [30]. Therefore, wave propagation takes place not only through the sound concrete and the epoxy filled crack but also through a zone of deteriorated material at both sides of the crack. The thickness of this zone is dependent on the aggregate size and for concrete with 20 mm aggregate it can be estimated at the order of 4–5 cm [30]. This is also the reason that the transit time of the longitudinal wave mentioned in the previous section is longer than expected even after impregnation.

In any case, the above results are a certain indication that the surface layer was filled in significant degree, to allow Rayleigh waves to propagate. Rayleigh measurements were repeated on the opposite side (bottom), and similar results were observed. Accordingly the propagation was restored showing that the epoxy material was sufficiently injected into the whole thickness of the structure although it was impregnated only from the upper surface.

4.2. Rayleigh dispersion curves

In search for powerful characterization tools, dispersion features have been increasingly studied recently [31–33]. Any inhomogeneity according to size parameters and properties, exhibits highlighted scattering influence at specific frequency bands and not the whole range. Therefore, the aim is to focus on these specific frequency bands that could supply more accurate information about the internal

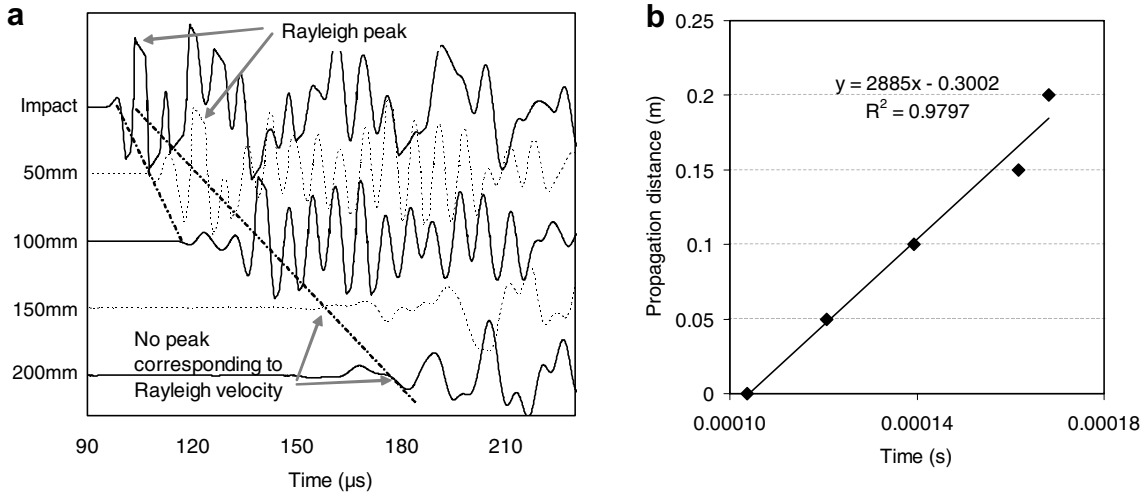

Fig. 7. (a) Waveforms of Fig. 6 (these corresponding to 150 mm and 200 mm are magnified by 20) and (b) correlation plot of distance to Rayleigh peak arrival time.

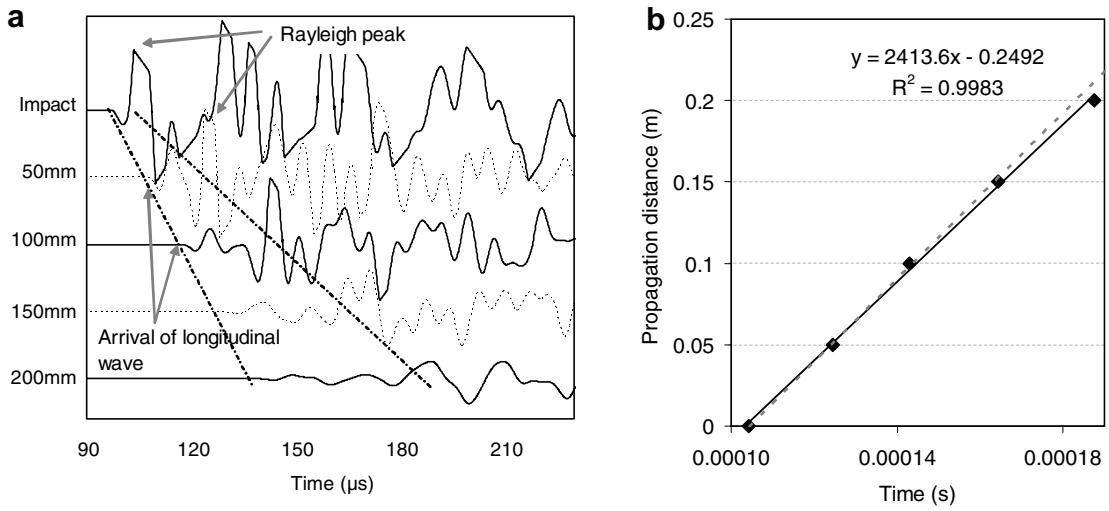

Fig. 8. (a) Waveforms of surface measurements at different propagation distances for concrete with epoxy filled crack at 125 mm and (b) correlation plot of distance to Rayleigh peak arrival time.

condition. Therefore, the dispersion curves of Rayleigh waves were calculated, using two signals collected at different points of the material. In the case of repaired material the sensors were placed in such a position that the epoxy filled crack was in between. The procedure involves the isolation of the part containing the clear Rayleigh cycle [34], conducting fast Fourier transform and calculating the phase difference between the two signals. The original procedure is described in [35]. In the examples of Fig. 9 the dispersion curves of sound and repaired material are presented. The observed trend for the sound material is in agreement with previous studies [31] showing that the phase velocity increases slightly with frequency for the band of 20–150 kHz. In the case of epoxy filled crack, the dispersion curve is translated lower by about 300 m/s. It is noted that it was not possible to obtain dispersion curve from the cracked stage (before repair with epoxy) since no Rayleigh peak was identified, as shown in Figs. 6 and 7. It is well known, as mentioned that for the Rayleigh waves, different frequencies correspond to different penetration depths, approximately similar to the wavelength. In this case, it seems reasonable that all the frequencies are delayed (lower curve for "repaired") due to the presence of the epoxy through the whole thickness of the deck. Therefore, horizontal propagation of Rayleigh waves on shallow as well as larger depths is influenced by the same vertical layer of the lower mechanical properties of the epoxy and are therefore delayed in a similar way. However, a higher discrepancy of the curves above 100 kHz can be noticed and it will be explored later in the analysis.

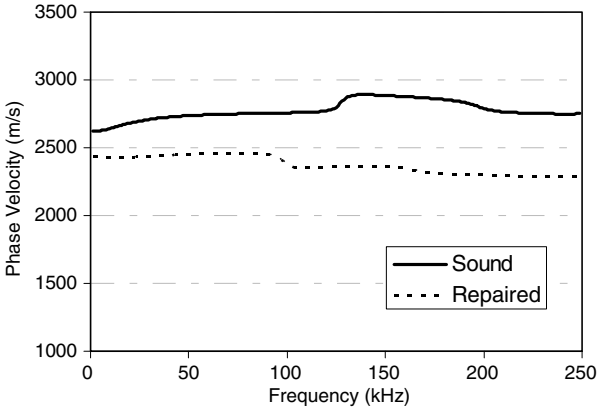

Fig. 9. Concrete phase velocity of Rayleigh waves vs frequency.

4.3. Frequency content and depth of penetration

One important parameter of Rayleigh waves is their frequency content, as mentioned above, that decides also their penetration depth and thus the layer that can be characterized with Rayleigh waves. The nature of these waves is non-dispersive [16,36], meaning that their propagation along a surface of a semi-infinite and homogeneous medium would not alter their frequency content and the velocity would not be frequency dependent. However, propagation in a non-homogeneous material like concrete is certainly dispersive for any kind of waves. A source of dispersion is the inhomogeneity of the material [17,37] containing a number of different phases, like sand, aggregates and voids that exist even in intact material. This dispersion is considered to be mainly due to scattering of the wavefront on these inhomogeneities and is studied in a number of cases [17,31–33,38,39]. The dispersion combined with the scattering attenuation and damping decreases the central frequency of a propagating Rayleigh wave, cutting off high frequency components. Consequently, the lower frequencies surviving correspond to longer wavelength and penetration depths.

Specifically, in Fig. 10a, the fast Fourier transforms of the responses at different points are depicted. Above 300 kHz the energy is negligible. The central frequency of

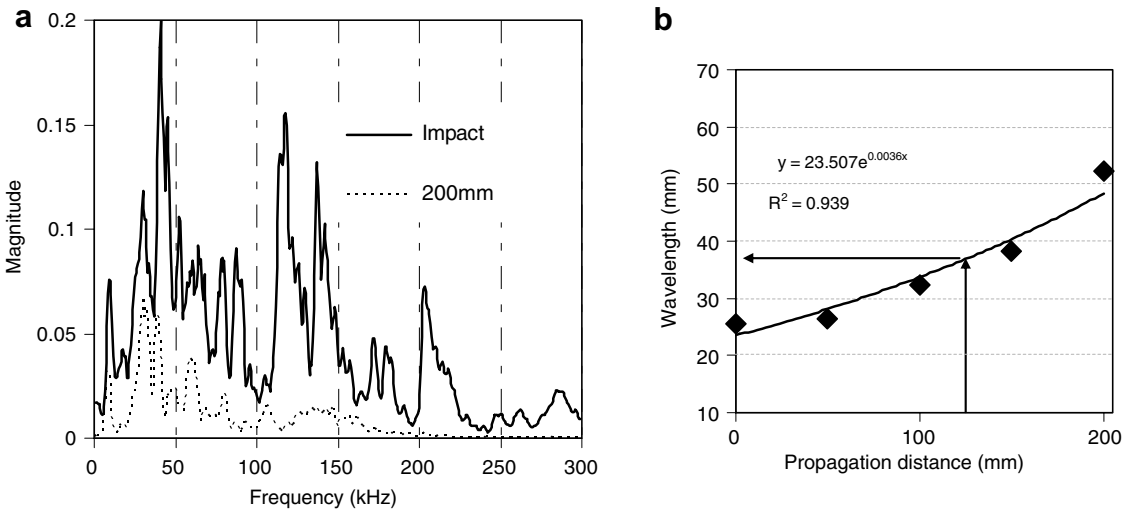

Fig. 10. (a) Fast Fourier transform of signals collected near the excitation point and 200 mm away and (b) wavelength of Rayleigh waves vs propagation distance for sound concrete.

the pulse measured exactly after the excitation, see impact in Fig. 10a, is about 115 kHz, while as obvious for the distance of 200 mm the frequency content is not only smaller but also translated to the lower frequencies. In order to exclude the possibly "ringing" behavior of the sensor it may be more reliable to focus only on the first strong Rayleigh peak in time domain. This peak gets broader with propagation as seen in Fig. 5a (t_1 and t_2). At the point of impact, the duration of the peak t_1 is approximately 4.4 μs, corresponding to period of 8.8 μs and a frequency of around 113 kHz. At the distance of 200 mm the peak is $t_2 = 11.6$ μs broad (period of 23.2 μs) corresponding to a central frequency of approximately 43 kHz. Therefore, using the peak duration of all five positions and considering a representative Rayleigh velocity of 2600 m/s, the average wavelength changes from about 23 mm to 50 mm after 200 mm of propagation through sound material, as seen in Fig. 10b. For the specific setup, in case of excitation at point 6, see Fig. 2, the propagation distance until the wavefront faces the crack is 125 mm. From the above it is realized that the representative penetration depth of Rayleigh wave at that point is of the order of 37 mm. This is an interesting quantification feature, since if the Rayleigh peak can be observed after the crack is repaired, it implies that the surface portion of 35–40 mm was substantially filled. It is noted however, as a limitation of Rayleigh application on structures with finite depth, that Rayleigh waves do not form at depths greater than half the beam depth as energy is distributed to other modes [20].

5. Tomographic reconstruction

As mentioned above, since there was access to both sides, the arrays of sensors were also used to produce tomography images of the interior. The previously mentioned approach with the Rayleigh offers information about the shallow portions of the crack. Tomography using two-side access was used to estimate the impregnation of the whole depth of the crack, by measuring the velocity of the area before and after repair. This is obtained from the combination of impact and receiving points, that results in a total of 50 wave paths perpendicular and diagonal that are sufficient to characterize the interior.

The tomography analysis aims at assigning a velocity value to each specific divided area (cell) of the cross section under examination. Two arrays of transducers were used, of five sensors each as shown in Fig. 2. The separation distance was 50 mm and excitation was conducted near each sensor that was used as a trigger for acquisition. In this case the recordings of the sensors on the opposite side are of interest.

5.1. Pulse velocity tomography

The wave transit time corresponding to each individual pair of transducers is dependent on the propagation velocity of the medium and the actual propagation path. Therefore, it is influenced by the presence of cracks or any other inhomogeneities. After each excitation, the transit time of the wave to each of the opposite side sensors is determined and applied to suitable software [40]. Therefore, the velocity structure of the element, namely tomogram, is calculated.

Applying this procedure to the cross section containing a crack before repair, it was quite visible that there was a significant discontinuity in the interior. In Fig. 11a one can observe the tomogram of the crack in hand. The yellow[1] colored area corresponds to a velocity of around 3500 m/s, being greatly influenced by the through-the-thickness crack. The tomography result gives also an insight of the internal pattern of the crack, due to the loop

[1] For interpretation of color in Figs. 11 and 13, the reader is referred to the web version of this article.

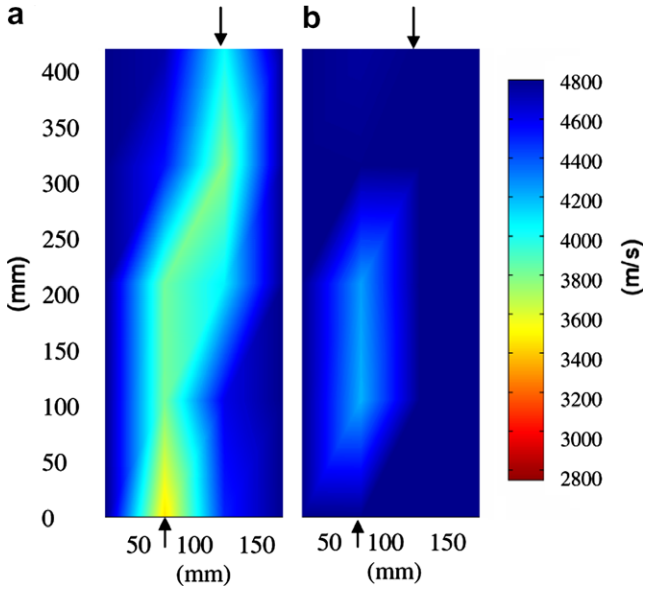

Fig. 11. Velocity tomograms of the vicinity of the crack (a) before and (b) after repair. The arrows correspond to the actual position of crack openings.

procedure employed for the calculation of the shortest path traveled in any case [40]. Indeed in the specific case, the top and bottom openings of the crack differ by 50 mm in horizontal distance. As seen, for some areas the crack decreased the apparent velocity to 70% of the intact state velocity.

In Fig. 11b, one can observe the tomogram of the same cross section after injection with epoxy. It is seen that wave propagation is facilitated and only some small tracks indicate the existence of crack that could be due to the fracture process zone that expands some cm from both sides of the crack, as mentioned earlier. Comparison of the image before and after, makes obvious that whatever discontinuity was initially present, was almost eliminated after repair, implying that the impregnation was successful. Most of the previously troublesome area seems thus eliminated, while a small remaining track of the discontinuity is related to a velocity of around 4200 m/s, 84% of the intact state, which is much elevated compared to the before repair situation. The same tomography procedure was applied to other cracks exhibiting in any case the much improved condition after impregnation.

5.2. Phase velocity tomography

The above approach concerns the transit time of the first detectable disturbance of the wave, corresponding to what is called pulse velocity. As previously applied for the surface measurement case, dispersion curves were now calculated for the through-the-thickness propagating wave. In this case the first peak is isolated, similarly to [31] and the same procedure with FFT and phase difference calculation is conducted. Examples of longitudinal wave phase

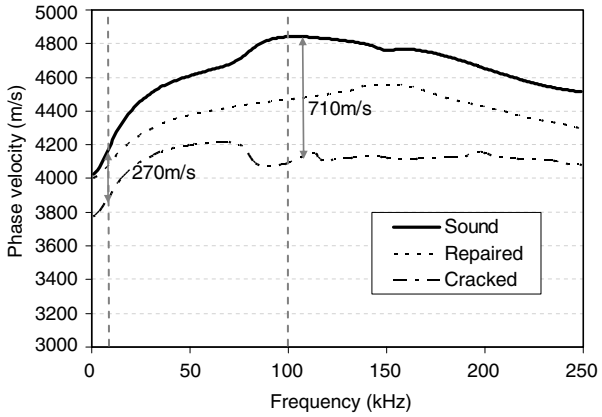

Fig. 12. Concrete phase velocity of longitudinal waves vs frequency.

velocities are depicted in Fig. 12. The specific curves are calculated from diagonal paths; 6–5, as seen in Fig. 2 for the cases of: sound material, path containing a crack and the same path after filling with epoxy. It is seen, similarly to the Rayleigh wave curves, that the velocity of sound material increases with frequency up to 100 kHz, while the cracked path results in much lower curve. Low frequencies around 10 kHz exhibit phase velocity of 3800 m/s, 270 m/s lower than the intact state. Correspondingly, frequencies at the vicinity of 100 kHz, present even greater discrepancy of more than 700 m/s (4100 for cracked and 4800 m/s for intact). The velocity of the repaired material is in any case in between. Since the velocity differences between the cracked, the repaired and the sound situation are not the same for each frequency component but seem to be highlighted for frequencies around 100 kHz, it was assumed reasonable to repeat the tomography procedure using velocities of different frequencies. Therefore, for all different wave paths (total number 50) between each impact point and receiver, the corresponding dispersion curve was calculated. Then for any selected frequency the corresponding phase velocity of all the wave paths was picked and fed to the tomography software. Herein, two indicative cases are discussed corresponding to lower and higher frequency bands acquired, namely 10 kHz and 100 kHz as seen in Fig. 12. In Fig. 13a and b one can observe the tomogram of the region of interest before and after the impregnation for 10 kHz, while Fig. 13c and d concern the case of 100 kHz. The frequency of 10 kHz corresponds to the low frequency limit of the acquisition setup and therefore, tomograms of lower frequencies are not presented although they can be obtained. On the other hand, after propagation through the deck of 419 mm the signal did not contain enough energy content above 100 kHz, therefore the use of higher frequency for tomography would result in questionable reliability. For both frequencies the repair effect is obvious, elevating the average velocity of the cells by 300 m/s for the case of 10 kHz and by about 450 m/s for 100 kHz. The areas showing the defect are substantially eliminated in both cases. However, the tomogram of 100 kHz seems more accurate concerning the location of

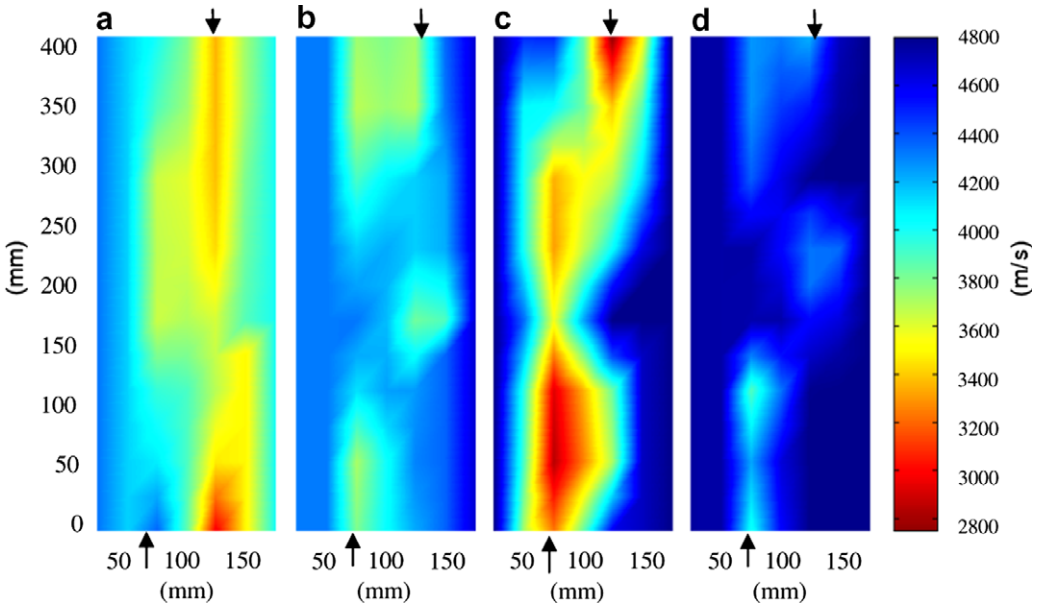

Fig. 13. Velocity tomograms of the vicinity of the crack for (a) 10 kHz before repair, (b) 10 kHz after repair, (c) 100 kHz before repair, and (d) 100 kHz after repair. The arrows correspond to the actual position of crack openings.

the defect, since as mentioned above, the crack in this case was not exactly vertical, but slightly inclined. Also, as the color variation implies, the difference of maximum to minimum for Fig. 13a is 31%, while for Fig. 13c the difference is 49%. This shows that, propagation at higher frequencies is more sensitive to the damage than lower frequencies. The interaction between inhomogeneity parameters, such as size and content, with stress wave velocity and attenuation is not easy to understand. However, in the specific case of this continuous through-the-thickness defect, the velocity of higher frequencies is more sensitive and therefore, appropriate for assessment of the repair effect. It is possible that much shorter wavelengths could interact more strongly with the crack thickness (or the epoxy layer after repair) leading to more accurate results. The inherent difficulty of this case, however, lies to the larger attenuation that makes the propagation of high frequencies troublesome.

6. Discussion

Using the above configurations it was possible to obtain very valuable information about the interior condition and the injection effect quickly and enable construction works to continue. The access to both sides in the case of bridge decks offers the possibility of applying arrays of sensors to examine thoroughly the interior, in addition to one-side measurements. The accurate characterization of the degree of filling of the crack volume with epoxy was not conducted. However, the tomography and Rayleigh analysis revealed that at least a substantial portion was impregnated, since the propagation in terms of velocity was mainly restored. In this case the information corresponds to the center line of the deck, see Fig. 2, top view, on the longitudinal axis of the structure. When time and logistics allow, many lines can be measured if there is concern about the non-symmetric effect of epoxy impregnation. Both pulse and phase velocity visualization proved adequate in such a configuration to indicate the damage, as well as, more importantly, the improvement effect after repair, and allow the construction to proceed.

6.1. Frequency considerations

Moreover, higher frequencies show greater potential for characterization, since they result in more highlighted discrepancies between damaged and intact state. It is generally accepted that short wavelengths are more suitable for characterization of defects in concrete. For concrete, in order to apply relatively short wavelengths, for example in the order of 10 mm, the frequency should be approximately 500 kHz. Although such a pulse can be excited, the attenuation would make the acquisition impossible at site. However, even in the limited applicable range of frequencies in this case, the exploitation of higher components, i.e. 100 kHz, seems more powerful than lower, i.e. 10 kHz. It is noted that the coherence function revealed that reliable results were obtained for the whole frequency range used for phase velocity calculation. This function is calculated through the autospectral and cross spectral densities of two signals and underlines the similarities in their frequency content. It is used in several cases for the processing of wave propagation data for assessment of reliability [21] or classification purposes [41,42]. In Fig. 14 one can observe the coherence function of surface signals for the case of sound, repaired and cracked material. It is obvious that for sound material the coherence function approaches unity up to the range of 300 kHz. For the case of repaired material great similarity

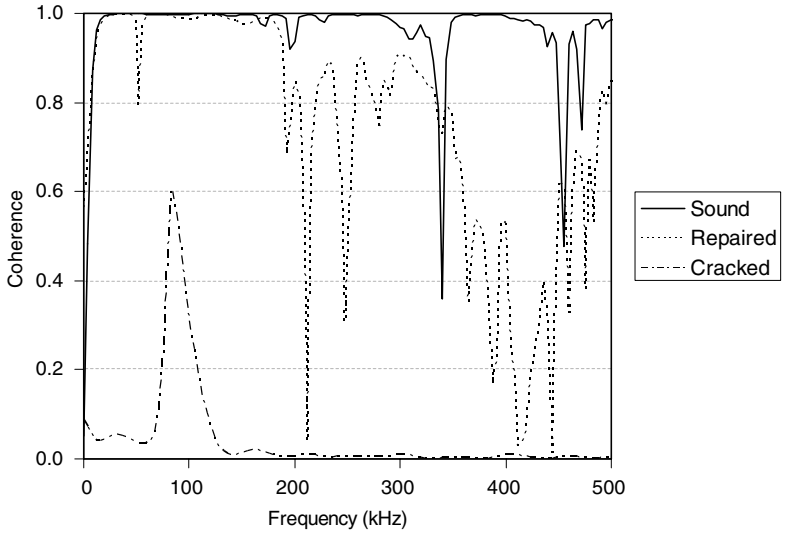

Fig. 14. Coherence function between signals collected at different states of concrete.

is observed up to 200 kHz. It is interesting to see that for the case of cracked material, due to the large thickness of the crack, the signal seems so distorted that the coherence function exhibits very low values for the entire range although there was no source of external noise.

6.2. Influence of reinforcing bars

From the tomography images it is obvious that there is no trace of steel reinforcement. There is a number of reasons making the tomogram insensitive to the rebar. Rebars of diameter 13 mm are present in two directions, parallel and vertical to the longitudinal axis. Stronger influence should be expected by the longitudinal reinforcement, as seen in Fig. 2 which is approximately vertical to all the wave beams. However, any wave beam passes through the same number of rebars. In Fig. 2 it is seen that after excitation, for example at position 5, the wave propagating to the opposite side sensors (i.e. 10, 9, 8, etc.) will face in any case two times reinforcement. Therefore, the influence to any different path, i.e. 5–8, 5–9 and 5–10, will be approximately the same and probably not distinguishable when compared to the influence of the crack that will definitely decrease the energy and velocity of path 5–8. Apart from this, the influence of the two rebars of 13 mm in the overall measured velocity of the 419 mm deck can be calculated to less than 1% [11]. Moreover, the major frequency of the excited wave is less than 100 kHz, corresponding to a wavelength of 45 mm, much longer than the rebar diameter making thus the propagation even more insensitive to the reinforcement. Finally, another important reason has to do with the tomography cell size. This is determined by the sensor arrangement (as mentioned 50 mm separation), which is much longer than the rebar diameter. Therefore, the reinforcement seems invisible due to its small size compared to the cell dimension, while on the other hand the continuous crack is clearly depicted. Reinforcement usually imposes restrictions to the depth characterization by one-side measurements [11,12]. In this case of through-the-thickness investigation however, the impregnation effect could be characterized clearly without being seriously masked by the existence of reinforcement.

6.3. Inspection of the shallow layer

In the tomography measurement many combinations of impact and receiving points lead, as mentioned, to a number of 50 different wave paths that are considered adequate for a cross section of 419 mm × 200 mm. However, due to the specific geometry, the interaction of the wave beams with the near surface portion of the crack is limited, as can be seen in Fig. 15. In fact, considering straight wave paths, the near the surface part of the crack, that is not crossed by any beam, is about 60–70 mm deep. Since the density of the wave beams is low for this shallow layer, Rayleigh waves analysis was also essential. At the cracked state, the identification of Rayleigh waves was not possible, as a result of the discontinuity. After application of epoxy, the Rayleigh wave propagation was restored and Rayleigh peaks were identified clearly. Such a behavior

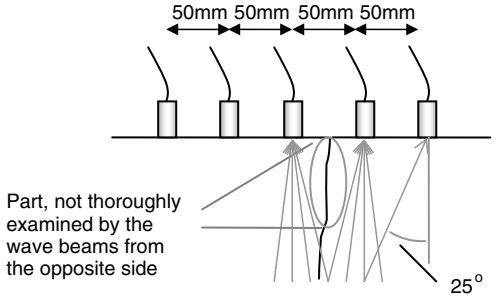

Fig. 15. Detail about interaction of wave beams with the near surface part of the crack.

demonstrated that at least a large portion of the surface layer of 35–40 mm was successfully filled, allowing the propagation of energy in the form of surface waves. In a big concrete structure this information obtained relatively easy and fast is considered adequate, although further detail should be desirable through more accurate correlations between the amplitude and frequency of the Rayleigh wave and the crack depth filled with epoxy. This would be of more importance in case there is no access to both sides. At that point the amplitude or frequency content of the Rayleigh waves should be used for the characterization of the crack from one side. Such correlations have been studied for metals [20] but for concrete there is still limited work [19,22]. Further investigation concerning the accurate characterization of the crack depth and degree of filling is currently undertaken by the authors combining numerical parametric study with experimental results of surface measurements on concrete material.

The use of an array of receivers (instead of using just two for example) enables the easier identification of the Rayleigh peak, as it can be tracked at a point that is very strong and followed along the propagation distance while being attenuated, as seen in Fig. 5a. Since the penetration depth of Rayleigh waves is similar to the wavelength, changing the excitation frequency could enable the characterization of different thickness of concrete. For example, in case the excited wavelength is totally blocked by the crack and the opposite side is not accessible, longer wavelength could be applied changing the excitation, see Fig. 16. This way a part of energy would be transmitted below the crack and more accurate evaluation could be feasible. The excitation frequency can be adjusted using different pulse generators, pencil lead break or ball impact of various diameters [6,8].

6.4. Amplitude considerations

Another feature that is expected to enhance characterization capabilities is the use of energy or amplitude parameters. This paper deals mainly with velocity analysis proving adequate to characterize the material. However, as is generally known, energy related parameters are more indicative of the damage than velocity [43,44]. In the particular case, since the crack was through the thickness, there was no detectable amplitude of Rayleigh. However, in other cases of partial surface opening cracks the amplitude and energy of the Rayleigh wave should be an important characteristic correlated to the crack depth. Also, concerning the through-the-thickness measurement, the adoption of energy features to a suitable attenuation tomography software could lead to highlighted differences between damaged and repaired state, provided that absolutely repeatable excitation and coupling conditions can be achieved. The sensor arrangement used herein, involves nominally a maximum angle of 25° for the most diagonal path of this case, see Fig. 15. Therefore, care should be taken for the angle of incidence. This should not have significant influence on the velocity measurement but some compensation should be necessary if amplitude analysis is to be undertaken.

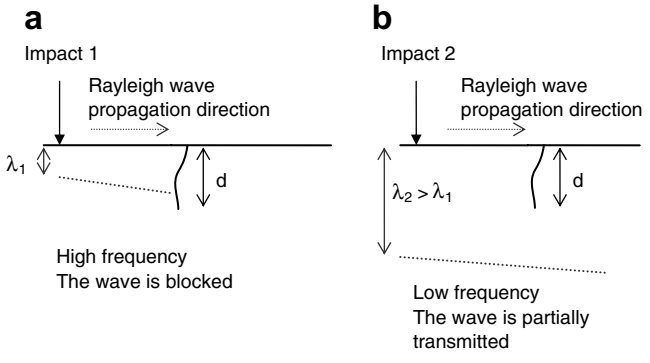

Fig. 16. Inspection with wavelength (a) shorter than the crack depth and (b) longer than the crack depth.

7. Conclusion

In the present work a relatively easy to apply methodology is proposed for evaluation of the repair effect at cracked bridge decks. Through-the-thickness cracks are common defects in bridges. The repair can be conducted by a suitable agent which is injected into the empty space sealing the crack. The repair effectiveness should be confirmed by means of a non-invasive technique. This is offered by the stress wave testing, using both Rayleigh surface waves and longitudinal waves propagating through the thickness of the structure when both sides are accessible. Examination by means of tomography, based on several paths of a cross section containing the crack, reveals quite evidently the impregnation of the empty volume previously occupied by the crack. This is due to the fact that filling the crack volume with epoxy reduces the transit time of wave propagation compared to the empty crack state. In this case, higher frequencies exhibit higher sensitivity and characterization capabilities. Due to the lower concentration of wave rays near the top and bottom surfaces, in order to increase the information concerning these shallow layers, application of surface waves is desirable to verify the filling near the surface. Thus, it is concluded that, for the characterization of through-the-thickness cracks as well as the repair effect, a tomographic approach with longitudinal waves can be used complementary to Rayleigh waves. Such a methodology can be applied easily and yield the necessary information about the efficiency of repair.

References

[1] Issa CA, Debs P. Experimental study of epoxy repairing of cracks in concrete. Constr Build Mater 2007;21:157–63.
[2] Wardany RA, Rhazi J, Ballivy G, Gallias JL, Saleh K. Use of Rayleigh wave methods to detect near surface concrete damage. In: 16th World conference on non destructive testing 2004 (WCNDT), Montreal, Canada, August 30–September 3, 2004.
[3] Hevin G, Abraham O, Pedersen HA, Campillo M. Characterisation of surface cracks with Rayleigh waves: a numerical model. NDT&E Int 1998;31(4):289–97.

[4] Ono K. Damaged concrete structures in Japan due to alkali silica reaction. Int J Cem Compos Lightweight Concr 1988;10(4):247–57.
[5] Kruger M. Scanning impact-echo techniques for crack depth determination. Otto-Graf-J 2005;16:245–57.
[6] Sansalone MJ, Streett WB. Impact-echo nondestructive evaluation of concrete and masonry. Ithaca, NY: Bullbrier Press; 1997.
[7] Shiotani T, Nakanishi Y, Iwaki K, Luo X, Haya H. Evaluation of reinforcement in damaged railway concrete piers by means of acoustic emission. J Acoust Emission 2005;23:260–71.
[8] Shiotani T, Aggelis DG. Damage quantification of aging concrete structures by means of NDT. In: Structural faults and repair-2006, Edinburgh, UK, June 13–15.
[9] Binda L, Modena C, Baronio G, Abbaneo S. Repair and investigation techniques for stone masonry walls. Constr Build Mater 1997;11(3):133–42.
[10] Thanoon WA, Jaafar MS, Razali M, Kadir A, Noorzaei J. Repair and structural performance of initially cracked reinforced concrete slabs. Constr Build Mater 2005;19(8):595–603.
[11] Malhotra VM, Carino NJ, editors. CRC handbook on nondestructive testing of concrete. Florida: CRC Press; 1991.
[12] Liu PL, Lee KH, Wu TT, Kuo MK. Scan of surface-opening cracks in reinforced concrete using transient elastic waves. NDT&E Int 2001;34:219–26.
[13] Doyle PA, Scala CM. Crack depth measurement by ultrasonics: a review. Ultrasonics 1978;16(4):164–70.
[14] Arias I, Achenbach JD. A model for the ultrasonic detection of surface-breaking cracks by the scanning laser source technique. Wave Motion 2004;39(1):61–75.
[15] Wu TT. Elastic wave propagation and nondestructive evaluation of materials. Proc Natl Sci Counc ROC(A) 1999;23(6):703–15.
[16] Graff KF. Wave motion in elastic solids. New York: Dover Publications; 1975.
[17] Owino OJ, Jacobs LJ. Attenuation measurements in cement-based materials using laser ultrasonics. J Eng Mech 1999;125(6):637–47.
[18] Jian X, Dixon S, Guo N, Edwards RS, Potter M. Pulsed Rayleigh wave scattered at a surface crack. Ultrasonics 2006;44:1131–4.
[19] Achenbach JD, Cheng A. Depth determination of surface-breaking cracks in concrete slabs using a self-compensating ultrasonic technique. In: Thompson DO, Chimenti DD, editors. Review of progress in quantitative nondestructive evaluation, vol. 15B. New York and London: Plenum Press; 1996. p. 1763–70.
[20] Edwards RS, Dixon S, Jian X. Depth gauging of defects using low frequency wideband Rayleigh waves. Ultrasonics 2006;44:93–8.
[21] Zerwer A, Polak MA, Santamarina JC. Detection of surface breaking cracks in concrete members using Rayleigh waves. J Environ Eng Geophys 2005;10(3):295–306.
[22] Wu J, Tsutsumi T, Egawa K. New NDT method for inspecting depth of crack in concrete using Rayleigh's wave. In: Symposium of Japanese Society of Non Destructive Inspection, Tokyo, 2003. p. 243–52.
[23] Kim DS, Seo WS, Lee KM. IE-SASW method for nondestructive evaluation of concrete structure. NDT&E Int 2006;39:143–54.
[24] Rhazi J, Hassaim M, Ballivy G, Hunaidi O. Effects of concrete nonhomogeneity on Rayleigh waves dispersion. Mag Concr Res 2002;54(3):193–201.
[25] Goueygou M, Piwakowski B, Fnine A, Kaczmarek M, Buyle-Bodin F. NDE of two-layered mortar samples using high-frequency Rayleigh waves. Ultrasonics 2004;42:889–95.
[26] Kase EJ, Ross TA. Quality assurance of deep foundation elements. In: 3rd International conference on applied geophysics – geophysics, Orlando, USA, December 8–12, 2003 [Florida Department of Transportation].
[27] Sassa K. Suggested methods for seismic testing within and between boreholes. Int J Rock Mech Mining Sci Geomech Abstr 1988;25(6):449–72.
[28] Yokota O, Takeuchi A. Injection of repairing materials to cracks using ultrasonic rectangular diffraction method. In: 16th World conference on non destructive testing 2004 (WCNDT), Montreal, Canada, August 30–September 3, 2004.
[29] Qixian L, Bungey JH. Using compression wave ultrasonic transducers to measure the velocity of surface waves and hence determine dynamic modulus of elasticity for concrete. Constr Build Mater 1996;4(10):237–42.
[30] Mihashi H, Nomura N, Niiseki S. Influence of aggregate size on fracture process zone of concrete detected with three dimensional acoustic emission technique. Cem Concr Res 1991;21:737–44.
[31] Philippidis TP, Aggelis DG. Experimental study of wave dispersion and attenuation in concrete. Ultrasonics 2005;43:584–95.
[32] Chaix JF, Garnier V, Corneloup G. Ultrasonic wave propagation in heterogeneous solid media: theoretical analysis and experimental validation. Ultrasonics 2006;44:200–10.
[33] Punurai W, Jarzynski J, Qu J, Kurtis KE, Jacobs LJ. Characterization of entrained air voids in cement paste with scattered ultrasound. NDT&E Int 2006;39(6):514–24.
[34] Dokun OD, Jacobs LJ, Haj-Ali RM. Ultrasonic monitoring of material degradation in FRP composites. J Eng Mech 2000;126(7):704–10.
[35] Sachse W, Pao YH. On the determination of phase and group velocities of dispersive waves in solids. J Appl Phys 1978;49(8):4320–7.
[36] Rahman M, Michelitsch T. A note on the formula for the Rayleigh wave speed. Wave Motion 2006;43:272–6.
[37] Jacobs LJ, Owino JO. Effect of aggregate size on attenuation of Rayleigh surface waves in cement-based materials. J Eng Mech—ASCE 2000;126(11):1124–30.
[38] Popovics S, Rose JL, Popovics JS. The behavior of ultrasonic pulses in concrete. Cem Concr Res 1990;20:259–70.
[39] Kim YH, Lee S, Kim HC. Attenuation and dispersion of elastic waves in multi-phase materials. J Phys D: Appl Phys 1991;24:1722–8.
[40] Kobayashi Y, Shiojiri H, Shiotani T. Damage identification using seismic travel time tomography on the basis of evolutional wave velocity distribution model. In: Structural faults and repair-2006, Edinburgh, UK, June 13–15, 2006.
[41] Philippidis TP, Aggelis DG. An acousto-ultrasonic approach for the determination of water-to-cement ratio in concrete. Cem Concr Res 2003;33:525–38.
[42] Grosse C, Reinhardt H, Dahm T. Localization and classification of fracture types in concrete with quantitative acoustic emission measurement techniques. NDT&E Int 1997;30(4):223–30.
[43] Shah SP, Popovics JS, Subramanian KV, Aldea CM. New directions in concrete health monitoring technology. J Eng Mech—ASCE 2000;126(7):754–60.
[44] Streeter K, Schuller M, Xi Y. Ultrasonic attenuation tomography of concrete structures. In: 16th Engineering mechanics conference (ASCE), Seattle, USA, July 16–18, 2003.